Simple method for real-time seismic damage assessment of bridges

Anastasopoulos, Ioannis; Anastasopoulos, P. Ch; Agalianos, A.; Sakellariadis, L.

Published in:
Soil Dynamics and Earthquake Engineering

DOI:
10.1016/j.soildyn.2015.07.005

Publication date:
2015

Document Version
Peer reviewed version

Simple method for real-time seismic damage assessment of bridges

Anastasopoulos, Ioannis; Anastasopoulos, P. Ch; Agalianos, A.; Sakellariadis, L.

Published in:
Soil Dynamics and Earthquake Engineering

DOI:
10.1016/j.soildyn.2015.07.005

Publication date:
2015

Simple method for real–time seismic damage assessment of bridges

by

I. Anastasopoulos[1], P.Ch. Anastasopoulos[2], A. Agalianos[3], and L. Sakellariadis[4]

Abstract

Seismic damage of bridges may pose a severe threat to motorway users, and preventive closure until post–seismic inspection may be viewed as the only safe option. However, such a measure may incur pronounced losses by obstructing transportation of rescue teams. On the other hand, allowing traffic on earthquake–damaged bridges is a difficult decision with potentially dire consequences. Hence, the main dilemma for the motorway administrator is whether to interrupt the operation of the network, calling for timely development and implementation of a RApid REsponse (RARE) system. The development of such a RARE system requires an effective means to estimate the seismic damage of motorway structures in real time. This paper contributes towards such a direction by introducing a simple method for real time seismic damage assessment of motorway bridges. The proposed method requires nonlinear dynamic time history analyses using multiple seismic records as seismic excitation. Based on the results of the analyses, statistical models are estimated, and nonlinear regression equations are developed to express seismic damage as a function of statistically significant intensity measures (IMs). Such equations are easily programmable and can be employed for real-time damage assessment, as part of an online expert system. In the event of an earthquake, the nearest seismic motion(s), recorded by an online accelerograph

[1] Professor, Division of Civil Engineering, University of Dundee; formerly National Technical University of Athens
[2] Assistant Professor, Department of Civil, Structural and Environmental Engineering, SUNY at Buffalo
[3] Civil Engineer, MSc, University of Dundee; formerly National Technical University of Athens
[4] Civil Engineer, MSc, University of Dundee; formerly National Technical University of Athens

network, will be used in real time to estimate the damage state of motorway structures, employing the developed equations. The efficiency of the proposed method is demonstrated using a single bridge pier as an illustrative example. Based on finite element (FE) analysis results, three nonlinear regression models are estimated correlating three damage indices (DIs) with statistically significantly IMs.

Keywords

Damage assessment; seismic vulnerability; real-time system; bridge pier; finite elements; nonlinear regression models; online architecture.

1. Introduction

Under normal conditions, the safety of motorway users is mainly related to the quality of the road network (road geometry, traffic characteristics, pavement condition) and the behavior of drivers [Anastasopoulos & Mannering, 2009, 2011; Anwaar et al., 2012; Anastasopoulos et al., 2012; Russo et al., 2014; Yasmin et al., 2014; Venkataraman et al., 2014]. In the event of a strong earthquake, the safety of motorway users is directly related to the seismic performance of motorway infrastructure. Structural damage, such as the bridge collapses of **Figs. 1a** and **1b** during the devastating 1994 Northridge [Hall, 1995; Basöz et al., 1999] and 1995 Kobe earthquakes [Kawashima & Unjoh, 1997; Hanshin Expressway, 1999], may pose a severe threat to the users of the transportation network as dramatically illustrated in **Fig. 1c**. In this particular case, a bus travelling on Hanshin Expressway No. 3 during the Kobe earthquake marginally stopped in front of collapsed bridge span. The consequences of a 14 m free-fall would have been detrimental to the bus and, most importantly, to its passengers.

Even if a motorway bridge is still standing after the main shock, it may be severely damaged and therefore prone to collapse when subjected to aftershocks [Franchin & Pinto, 2009]. Preventive closure of the motorway until post–seismic inspection may seem as the safest option. However, such closure will unavoidably lead to serviceability deterioration (**Fig. 1d**), and may also incur pronounced losses by obstructing transportation of critical groups, such as rescue teams. In addition, such an action would prevent the use of the motorway as an evacuation path. On the other hand, allowing traffic on earthquake–damaged bridges is a difficult decision with potentially dire consequences. Maintaining the network in operation without inspection may jeopardize the safety of users and rescue teams, since some structures may already be at a critical state. Hence, the main dilemma for the motorway administrator will be whether to interrupt the operation of the network.

But even if structural damage is not substantial, the lack of coordinated action on behalf of the Motorway Administrator may increase the feeling of insecurity and resentment to the motorway users. This can in turn increase the generalized sense of panic, and further disrupt the operation of the network, or even result in additional injuries (or even worse, fatalities). Although the direct consequences of a strong earthquake cannot be easily avoided (as they would probably require substantial expenditure for rehabilitation), the indirect consequences can be effectively mitigated through timely development and implementation of a RApid REsponse (RARE) system. The objectives of such a RARE system are: (a) to ensure the safety of motorway users and minimize the levels of distress, (b) to minimize closure of the motorway, and (c) to optimize the post-seismic serviceability of the motorway.

Several emergency response systems have been developed worldwide [e.g., Erdik et al., 2011]. Such systems can be classified with respect to the scale of the reference area as global or local. Apart from major global earthquake management systems, such as the Global

Disaster Alert and Coordination System [GDACS, www.gdacs.org; De Groeve et al., 2006] and WAPMERR [www.wapmerr.org], several local systems have been developed to estimate the damage and casualties in near–real time for large cities such as Tokyo, Istanbul, and Naples [Erdik et al., 2003]. The majority of such systems employ recordings from strong motion networks to characterize seismic events and estimate the damage by use of known inventory of elements exposed to hazard and associated vulnerability relationships. With respect to transportation networks, there have been some attempts to apply seismic risk assessment to motorway systems such as the one in the Friuli-Venezia Giulia region of NE Italy [Codermatz et al., 2003].

Despite the considerable work on the subject, to the best of the authors' knowledge, there are no documented efforts to develop a RApid REsponse system for motorway networks. The development of such a RARE system requires an effective means to estimate the seismic damage of motorway components (such as bridges, tunnels, retaining walls, cut slopes, and embankments) in real time, immediately after the occurrence of a seismic event, which is the scope of the present paper. Such real time estimation of the seismic damage is of the utmost importance: (i) to rationally decide whether there is a need for emergency inspection, and (ii) to rationally allocate inspection teams, allowing for minimum disruption of traffic operations and optimization of post-seismic motorway serviceability. The paper applies an inter-disciplinary approach, combining finite element (FE) simulations with statistical modeling.

2. Overview of the RARE System

A RARE system is currently being developed as part of a European research project, using the Attiki Odos Motorway (Athens, Greece) as a case study. The detailed description of the system is not within the scope of this paper, but a brief overview is considered necessary to put the work presented herein into context. The four main steps that are required for the preparation (before the earthquake) of the RARE system are sketched in **Fig. 2**.

First of all (Step 1), a comprehensive GIS database of the motorway network is required, including all the necessary information to describe the motorway and its key components: geographic distribution; location of the various structures; typologies; geotechnical, tectonic and topographic conditions; and traffic capacities. Moreover, a carefully-documented database of motorway structures is essential, focusing on the most commonly observed typologies of each element at risk (bridges, cut-and-cover and bored tunnels, retaining structures, cut slopes, and embankments). If resources were unlimited, each motorway structure could be equipped with a state-of-the-art monitoring system, which could provide a direct assessment of the seismic damage.

An alternative is to install a network of accelerograph stations (Step 2), which will record the seismic motions at characteristic locations along the motorway. The latter will be used as the basis to estimate the expected seismic damage employing the proposed rapid damage assessment system. The design of such an online architecture requires strategically optimized selection of station locations, calling for a trade-off between the installation cost and the quality of real-time data (i.e., the seismic records). Obviously, an adequately large number of instruments is required in order to ensure adequate geographic coverage. The locations and the distribution of the instruments should be decided accounting for local site conditions and potential 2D (topography and/or valley) effects. Both can have a significant effect on the ground motion (amplification or de-amplification), and may therefore alter the performance of a motorway bridge. Moreover, if allowed by the available budget, it would be desirable to install some of the instruments in the vicinity of major motorway bridges.

Then (Step 3), for each class of structures, nonlinear dynamic time history FE analysis is performed using multiple seismic records as seismic excitation. Each record is scaled to PGA ranging from 0.1 to 1.2 g (or more, if necessary). The output of the numerical analysis is the damage of the structure as a function of the seismic excitation. The damage is expressed with one or more damage indexes, such as the drift ratio δ_r. The latter has been identified as an appropriate damage index in many studies, as it provides a direct indication of the damage condition of a structure [Çelebi et al., 2004; Çelebi, 2008]. Finally (Step 4), for all seismic excitations the corresponding intensity measures (*IMs*) are computed, and based on the results of the FE analyses a dataset correlating one or more damage indexes with *IMs* is developed. The latter is then used to develop statistical models, expressing the seismic damage (using one or more of the damage indexes) as a function of the most statistically significant IMs.

As schematically illustrated in **Fig. 3**, in the event of an earthquake, the real-time system will record seismic accelerations at various locations along the motorway. This way, the seismic excitation will be available in real time, right after the occurrence of the seismic event. Naturally, the accuracy of the damage assessment will be a function of the density of the accelerograph stations, which is of course related to the available resources. For each structure, the nearest record(s) will be used to assess the seismic damage employing the simplified approximate method of this paper. Soil–structure interaction (SSI) may have a significant effect on the seismic damage of a bridge, and should be taken into account. Such a simplified method accounting for SSI is presented in Anastasopoulos et al. [2015].

As discussed in more detail in the next section, the proposed method estimates the damage state (e.g., no essential damage, relatively small damage, serious damage, severe damage up to collapse) on the basis of easily programmable equations. The latter correlate the damage state with a number of statistically significant intensity measures (IMs), which are easily programmable to be computed in real time for the nearest record(s). For each structure or class of structures, the nonlinear regression equations are estimated making use of FE simulations. In the next section, the proposed methodology is presented and discussed using a simple bridge structure as an illustrative example.

3. Outline of the Proposed Method

Fragility curves are widely used to assess the seismic vulnerability of infrastructure. They relate the probability of an element at risk to reach or exceed a damage state with the seismic intensity, typically expressed by a seismic intensity measure (IM) such as the peak ground acceleration (PGA), velocity (PGV), or displacement (PGD). An example of fragility curves for reinforced concrete (RC) and steel girder bridges is shown in **Fig. 4a**, adapted from Nielson & DesRoches [2007a]. Fragility curves can be broadly categorized as: (a) generic, based on expert judgment [e.g., ATC-13, ATC-25]; (b) empirical, based mainly on surveys after strong earthquakes [Yamazaki et al., 1999; Basoz et al., 1999; Shinozuka et al., 2000a; Kiureghian, 2002]; and (c) analytical, based on numerical simulations [Shinozuka et al., 2000b; Karim & Yamazaki, 2001; Elnashai et al., 2004; Nielson & DesRoches, 2007b]. A comprehensive review of the state of the art on the subject can be found in Pitilakis et al. [2014] and Pitilakis & Crowley [2014].

Another approach to assess the seismic vulnerability of a structure is Incremental Dynamic Analysis (IDA), according to which the numerical model of the structure is subjected to one or more seismic excitations, progressively scaled to different levels of increasing intensity [Vamvatsikos & Cornell, 2002]. This way IDA curves are produced, correlating a damage index (DI) with an IM. An example of such an IDA curve is presented in **Fig. 4b**, adapted from Vamvatsikos & Cornell [2002]. The concept, which had been earlier mentioned by Bertero [1977], has also been adopted by FEMA [2000].

Recognizing that PGA and PGV are poor indices of seismic intensity, a variety of intensity measures have been proposed by various researchers, such as the Housner Intensity [Housner, 1952] and the Arias Intensity [Arias, 1970]. Although such IMs are certainly much more efficient, the correlations of the seismic damage are not always adequate [Garini & Gazetas, 2013]. It seems that a single IM is possibly not adequate to capture all of the characteristics of a seismic motion. In this paper, instead of trying to come up with an optimum IM, statistical modeling is employed to combine an appropriate number of statistically significant IMs. To the best of the authors' knowledge, this has not been attempted before and can be of relevance especially within the context of the present study, as the seismic excitation will be known (having been recorded by the nearest accelerograph) just after the occurrence of the seismic event. This knowledge of the seismic excitation constitutes a major difference to the traditional (a priori) risk assessment, in which case the seismic excitation cannot possibly be predicted, and hence probabilistic approaches considering a variety of seismic sources are certainly more appropriate.

3.1 Problem definition and FE modelling

In order to demonstrate the efficiency of the proposed method, a single bridge pier is used as an illustrative example (**Fig. 5**), inspired by the Fukae bridge which collapsed during the 1995 Kobe earthquake [Anastasopoulos et al., 2010]. The deck, of mass m = 1200 Mgr is supported by a RC pier of height h = 12 m and diameter d = 3 m (**Fig. 5a**). The pier is designed according to the Greek Seismic Code [EAK 2000] for design acceleration A = 0.24 g, considering a behavior factor q = 2. The elastic fixed-base period is T = 0.48 sec, yielding design spectral acceleration SA = 0.3 g, and design bending moment $M_D \approx 43$ MNm. As shown in **Fig. 5b**, a longitudinal reinforcement of 100 d_{bL} = 32 mm bars (100Φ32) is required, combined with d_{bw} = 13 mm hoops spaced at 8 cm.

The seismic performance of the bridge is simulated employing the FE method, using the numerical code ABAQUS. The behavior of the RC pier is simulated with an appropriately calibrated kinematic hardening model with a Von Mises failure criterion and associative flow rule. Although the model is mainly intended to stimulate the inelastic behavior of metals subjected to cyclic loading, its parameters can be calibrated to match the moment–curvature (M–c) response of the RC pier [Gerolymos et al., 2005]. The bending moment of a circular section is by definition related to the normal stresses σ as follows:

$$M = 2\int_0^{\Pi}\int_0^{d/2} \sigma r^2 \sin\theta \, dr d\theta \tag{1}$$

For the maximum yield stress σ_y this relationship yields:

$$M_y = \frac{1}{6}\sigma_y d^3 \tag{2}$$

The maximum yield stress according to the kinematic hardening model is given by the following expression:

$$\sigma_y = \frac{c}{\gamma} + \sigma_0 \tag{3}$$

where the initial kinematic hardening modulus c is equal to the modulus of elasticity E. To simulate the descending branch, after the ultimate ductility capacity is reached, a user subroutine is encoded in ABAQUS. The parameters of the model are calibrated against the results of RC section analysis using the USC_RC software [2001]. The result of the calibration procedure is shown in **Fig. 5c**.

The seismic performance of the bridge is investigated through nonlinear dynamic time history analysis. In order to cover a wide range of strong motion characteristics, 29 real records from earthquakes of various intensities and kinematic characteristics are used as seismic excitation. The selected records along with their elastic acceleration response spectra and the design spectrum are presented in **Fig. 6**. In a way similar to IDA, each record is scaled to PGA ranging from 0.1 g to 1.2 g, yielding a dataset of 347 seismic excitations.

3.2 Correlation of Seismic Damage with Intensity Measures

Based on the results of the FE analyses, three different damage indices (DIs) are used to express the seismic damage of the bridge pier:

(a) The maximum drift ratio, $\delta_{r,max}$ (%):

$$\delta_{r,max} = \frac{\delta_{max}}{h} * 100\% \tag{4}$$

where δ_{max} is the maximum lateral deck displacement and *h* is the height of the pier;

(b) The residual drift ratio, $\delta_{r,res}$ (%):

$$\delta_{r,res} = \frac{\delta_{res}}{h} * 100\% \tag{5}$$

where δ_{res} is the residual lateral deck displacement and *h* is the height of the pier; and

(c) The ratio of ductility demand over ductility capacity, μ_d/μ_c.

In order to assess the seismic damage of the pier, influential factors affecting the three DIs are identified, through estimation of three nonlinear regression models, as discussed in the next section. As explanatory parameters, the IMs that statistically significantly affect the DIs are used. In contrast to past research that has investigated the correlation between a DI and one IM at a time, the presented statistical models identify the causal relationships instead, accounting simultaneously for all possible factors that can have an effect on the expected values of the DIs. On one hand, this allows for accurately forecasting expected values of the DIs (something that cannot be achieved through a correlation coefficient), while on the other hand the true unmasked effects of all statistically significant causal factors (i.e., IMs) are captured.

A total of 19 popular IMs found in the literature [e.g., Garini & Gazetas, 2013] are selected for analysis. These are computed for all (347) seismic excitations, yielding a dataset of the 3 DIs (FE analysis output) as a function of the 19 IMs (computed directly). It is emphasized that the same analysis can be conducted using a different, possibly more sophisticated, FE model and/or a different set of IMs. The purpose of this paper is to demonstrate the efficiency of the proposed method in a relatively simple manner. Brief definitions of the 19 DIs are as follows:

- The peak ground motion values of acceleration *PGA*, velocity *PGV,* and displacement *PGD*.
- The Arias Intensity, I_A, is proportional to the integral of the squared acceleration $A(t)$ time history [Arias, 1970]:

$$I_A = \frac{\pi}{2g} \int A^2(t)dt \tag{6}$$

- The Housner Intensity, I_H, is the integral of the pseudo-velocity response spectrum over the period range 0.1 to 2.5 sec [Housner, 1952]:

$$I_H = \int_{0.1}^{2.5} PS_V(T, \xi = 5\%)dT \tag{7}$$

- The RMS acceleration, A_{RMS}, is the square root of the mean of the acceleration $A(t)$:

$$A_{RMS} = \sqrt{\frac{\int A^2(t)dt}{T_D}} \tag{8}$$

where T_D : the duration of the record.

- The RMS velocity, V_{RMS}, is the root mean square of the velocity record $V(t)$:

$$V_{RMS} = \sqrt{\frac{\int V^2(t)dt}{T_D}} \tag{9}$$

- The RMS displacement, D_{RMS}, is the root mean square of the displacement record $D(t)$:

$$D_{RMS} = \sqrt{\frac{\int D^2(t)dt}{T_D}} \tag{10}$$

- The Characteristic Intensity, I_C, is defined as:

$$I_C = (A_{RMS})^{3/2}\sqrt{T_D} \tag{11}$$

- The Specific Energy Density, S_E, is defined as:

$$S_E = \frac{V_S \rho_S}{4}\int V^2(t)dt \tag{12}$$

where V_S : the shear wave velocity and ρ_s : the mass density.

- The Cumulative Absolute Velocity, *CAV*, is defined as:

$$CAV = \sum_{i=1}^{N} H(PGA_i - A_{min}) \int_{t_i}^{t_{i+1}} |A(t)|dt \tag{13}$$

where N is the number of the 1-second time windows in the time series, PGA_i is the PGA (normalized by g) during time window i, t_i is the start time of the time window i, A_{min} is an acceleration threshold (user-defined, usually taken as 0.025g) to exclude low amplitude motions contributing to the sum and *H(x)* is the Heaviside step function (unity for x>0, zero otherwise).

- The Sustained Maximum Acceleration, *SMA*, is the third highest absolute peak in the acceleration time history [Nuttli, 1979].
- The Sustained Maximum Velocity, *SMV*, is the third highest absolute peak in the velocity time history [Nuttli, 1979].
- The Acceleration Spectrum Intensity, *ASI*, is calculated from the spectral acceleration [Von Thun et al., 1988]:

$$ASI = \int_{0.1}^{0.5} S_A(5\% , T)dT \tag{14}$$

- The Velocity Spectrum Intensity, *VSI*, is calculated from the spectral velocity [Von Thun et al., 1988]:

$$VSI = \int_{0.1}^{2.5} S_V(5\%, T)dT \quad (15)$$

- The Acceleration parameter, A_{95}, is the level of acceleration which contains up to 95% of the Arias Intensity [Sarma & Yang, 1987].

Some additional parameters are often used as indices of destructiveness. These include: (a) the Predominant Period, T_P, which is estimated using the 5% damped acceleration response spectrum at its maximum (as long as T_P > 0.2 s); (b) the Significant Duration, D_{sig}, which is the interval of time between the accumulation of 5% and 95% of Arias Intensity; and (c) the Mean Period, T_{mean}, which is obtained from the Fourier amplitude spectrum as:

$$T_{mean} = \frac{\Sigma(\frac{{C_i}^2}{f_i})}{\Sigma {C_i}^2} \quad (16)$$

where C_i is the Fourier amplitude for each frequency f_i within the range 0.25-20 Hz.

4. Investigation of the Effectiveness of a single IM

The results of the FE simulations are aggregated and classified in a database including the 3DIs as a function of the 19 IMs for each one of the 347 acceleration time histories [Agalianos & Sakellariadis, 2013]. Excel trend-lines are used between a single DI and a single IM. The resulting graphs aim to show the correlation between a specific DI and a specific (single) IM.

Typical graphs that show this correlation as obtained from the analyses are shown in **Figs. 7** and **8**. From these graphs it becomes evident that a single IM is a poor index of the seismic damage of the pier, as expressed through the DIs. For example, **Fig. 7a** shows the correlation of $\delta_{r,max}$, as obtained from the FE analysis, with the Arias Intensity I_A. Observe that for I_A = 5 m/s, the maximum drift ratio $\delta_{r,max}$ varies from less than 1 (minor damage) to more than 5 (collapse). The same applies to the correlation of $\delta_{r,max}$ with I_A (**Fig. 7b**), but also the correlation of $\delta_{r,res}$ with I_H (**Fig. 8a**) and of μ_d/μ_c with A_{rms} (**Fig. 8b**). The obtained results are quite similar for all possible combinations between DIs and IMs. Therefore, it can be concluded that a single IM cannot be used to predict the structural damage, even for this very simple case of a SDOF system.

5. Nonlinear Regression Models of Damage Indexes

As discussed above, predicting a DI on the basis of an Excel trend line using a single IM is inefficient. Even in the case that such an approach may provide reasonable results, the true unmasked effect of the IM on the DI is not captured. In fact, this could be an artifact of the data, as the IM will most likely be capturing the effect of other omitted explanatory parameters (e.g., other statistically significant IMs), masked behind its estimated coefficient. This omitted variables bias [see Washington et al., 2011], is a serious misspecification error that occurs when omitted independent variables are correlated with an included independent variable, and leads to biased parameter estimates, and in turn to erroneous inferences and inefficient estimators. It is therefore of great importance to provide well specified models that can predict the DIs, in terms of all statistically significant IMs.

For model building, attention is given to all regression properties, such as heteroscedasticity, autocorrelation, exogeneity of the regressors, etc. [see Washington et al., 2011]. As the dependent variables (the DIs) can only take positive values, an exponential relationship is assumed between the dependent variables and the regressors (the IMs). Note that in any other case, negative values for the dependent variables (the DIs) could also –theoretically– be predicted, which would be invalid. Regardless, the exponential transformation further allowed us to have models with better overall statistical fit and improved forecasting accuracy as compared to the linear regression model alternatives (where the relationship between the damage indices and the intensity measures are strictly linear). To that end, nonlinear regression models are estimated for each DI, and all IMs are tested for inclusion in the model. The nonlinear regression models are of the form:

$$Y_i = EXP[\beta_0 + \beta_1 * X_{1\iota} + \varepsilon_i] \tag{17}$$

where, Y_i is the dependent variable (i.e., the damage indices) which is a function of a constant term β_0 and a constant β_1 times the value X_1 of independent variable X (i.e., the IMs) for observation i (i = 1, 2, ..., n) plus a disturbance term ε.

Furthermore, all explanatory parameters included in the models are statistically significant at 0.90 level of confidence (with most of them being statistically significant at 0.99 level of confidence). Finally, the effect of an IM on the DI may not be of a linear form. Hence, several transformations (power forms, logarithmic relationships, etc.) were tested, with the ones presented below, providing the best statistical fit and forecasting accuracy potential. The resulting nonlinear regression model equations for the three DIs are as follows:

$$\delta_{r,\max} = \mathrm{EXP}\begin{bmatrix} 0.70612*\mathrm{LN(PGA)} + 12.97257*\frac{1}{\mathrm{PGV}} - 2.50142*\frac{1}{\sqrt{\mathrm{PGD}}} - 3.18861*{A_{RMS}}^2 + \\ +1.46808*\frac{1}{\sqrt{D_{RMS}}} - 0.18791*\frac{1}{\sqrt{I_C}} - 11.8121*\frac{1}{\sqrt{S_E}} + 212.77053*\frac{1}{\mathrm{CAV}} + \\ + 0.10551*\sqrt{\mathrm{VSI}} - 0.04486*\sqrt{H_I} - 0.02203*\frac{1}{\mathrm{SMA}} + 3.05564*\frac{1}{\mathrm{SMV}} + \\ + 0.1741*\mathrm{LN}(T_P) - 0.28233*\frac{1}{\mathrm{T}_{mean}} + 0.18476*\sqrt{D_{sig}} \end{bmatrix} \tag{18}$$

$R^2_{adjusted} = 0.949$

$$\delta_{r,res} = \mathrm{EXP}\begin{bmatrix} 3.43909*\sqrt{\mathrm{PGA}} + 21.66195*\frac{1}{\mathrm{PGV}} - 0.00013519*\frac{1}{{A_{RMS}}^2} - \\ - 0.13401*\mathrm{LN}(\mathrm{D}_{RMS}) - 0.22024*I_A - 4.25419*\sqrt{\mathrm{I}_c} + \\ +0.00187*\mathrm{CAV} - 0.5073*\frac{1}{\sqrt{\mathrm{ASI}}} - 37.86229*\frac{1}{\sqrt{\mathrm{VSI}}} + 0.00000591*{I_H}^2 - \\ - 2.10909*\sqrt{\mathrm{SMA}} + 5.63051*T_P - 4.13821*{T_P}^2 - 1.31971*\frac{1}{\sqrt{D_{sig}}} \end{bmatrix} \tag{19}$$

$R^2_{adjusted} = 0.913$

$$\frac{\mu_d}{\mu_c} = \mathrm{EXP}\left[\begin{array}{c} 3.48948*\sqrt{\mathrm{PGA}} + 7.75634*\frac{1}{\mathrm{PGV}} - 2.69217*\frac{1}{\mathrm{PGD}} - 10.19223*{A_{RMS}}^2 + \\ +1.06649*\frac{1}{\sqrt{D_{RMS}}} + 2.34031*\sqrt{\mathrm{I}_c} - 30.07042*\frac{1}{{S_E}^2} + 7037.14915*\frac{1}{\mathrm{CAV}^2} - \\ - 38.85989*\frac{1}{\sqrt{\mathrm{VSI}}} + 78.64505*\frac{1}{I_H} - 0.00024402*\frac{1}{\mathrm{SMA}^2} + \\ + 0.00000964*\mathrm{SMV}^2 - 0.87646*{A_{95}}^2 - 1.51743*\frac{1}{\sqrt{T_{mean}}} \end{array}\right] \quad (20)$$

$R^2_{adjusted} = 0.963$

The models' overall statistical fit can be assessed through the Adjusted R-squared, as follows:

$$R^2_{adjusted} = 1 - [(n-1)/(n-p)] * \left[\left(\sum_{i=1}^{n}\left(Y_i - \hat{Y}_i\right)^2\right)/\left(\sum_{i=1}^{n}(Y_i - \bar{Y})^2\right)\right] \quad (21)$$

where Y and $\hat{Y}$ are the observed and predicted values, respectively, of the dependent variable (i.e., DI) for observation i (i = 1, 2, …, n), $\bar{Y}$ is the observed mean value of the dependent variable, and p is the number of explanatory model parameters.

This goodness-of-fit measure gives a relative illustration of how much the estimated model explains the variance in the data, accounting for the number of parameters. This makes the Adjusted R-squared a robust goodness-of-fit measure when comparing models with different number of parameters.

6. Efficiency of the nonlinear regression model equations

The efficiency of each one of the three developed nonlinear regression model equations is examined comparing the predicted structural damage of the SDOF system by using the corresponding equation to the observed one, as obtained from the numerical analysis. **Figure 9** presents the observed and the predicted structural damage for each one of the three DIs, as well as the average deviations and the mean absolute percentage error (MAPE). The latter can be estimated as follows:

$$MAPE = \frac{1}{n}\sum_{i=1}^{n}|PE_i| \quad (22)$$

where $PE_i = 100\% \left(Y_i - \widehat{Y_i}\right) / Y_i$ is the percentage error for observation *i* of the actual damage index value *Y*, and the model-estimated damage index value $\widehat{Y_i}$, for observation *i*.

The resulting MAPE values give the percentage that the predictors under- or over-estimate the observed values, on average. From these results it can be concluded that the nonlinear regression model equations for predicting structural damage reduce significantly the deviations between the predicted results and the observed ones from the numerical analysis. These deviations are considered acceptable for the purposes of a Rapid Response System.

The efficiency of the nonlinear regression model equations is shown more clearly in **Figs. 10** to **12**. In these figures the observed damage states of the numerical analysis are compared to the predicted ones using the nonlinear regression model equations for the three DIs and for all 29 historic earthquake records. The damage states considered are based on typical values of drift ratio and μ_d/μ_c for each damage state with reference to Response Limit States [Priestley et al. 1996]. In these figures, it is also shown on how many of the total of the 347 dynamic analyses the observed damage state is the same with the predicted one, on how many there is one state difference between them and on how many there is two states difference (error). As illustrated in **Fig. 10**, when examining the maximum drift ratio $\delta_{r,max}$, the nonlinear regression equations correctly predict the damage state in 84% of the examined cases, having a one state difference in the remaining 16%. The performance is slightly worse when examining the residual drift ratio $\delta_{r,res}$ (**Fig. 11**), as the correct prediction rate is 81%, and there a two-state difference is observed in 1.7% of the examined cases. As summarized in **Fig. 12**, the situation is similar when μ_d/μ_c is used as a damage index, and hence it may be concluded that the most reliable prediction can be made on the basis of $\delta_{r,max}$.

The following step is to examine the efficiency of the developed nonlinear regression model equations on out-of-sample earthquake records. To that end, a set of 15 different historic records is used to perform a new series of nonlinear time history analyses in order to obtain the DIs and compare them to the relevant results of the equations. In **Figure 13** the observed damage states of the numerical analysis are compared to the predicted ones using the nonlinear regression model equation for μ_d/μ_c and for the 15 out-of-sample historic records. It is also shown on how many of the total of 15 dynamic analyses the observed damage state is the same with the predicted one, on how many there is one state difference between them and on how many there is two states difference (error). In general terms it is observed that the nonlinear regression model equations constitute a satisfactory way to estimate the structural damage of SDOF systems, as far as a Rapid Response System is concerned.

7. Synopsis and Conclusions

The paper has introduced a simple method to estimate the seismic damage of motorway bridges in real time, immediately after the occurrence of a seismic event. The work presented herein is part of an ongoing research effort aiming towards the development of a RApid REsponse (RARE) system for metropolitan motorway networks. A cross-disciplinary approach has been applied, combining FE simulations with statistical modeling. The proposed method requires nonlinear dynamic time history analysis using multiple seismic records. Based on the results of the FE simulations, statistical modeling is applied to develop nonlinear regression model equations, expressing the seismic damage as a function of statistically significant intensity measures (IMs).

The efficiency of the proposed method was demonstrated using a single bridge pier as an illustrative example. A total of 29 real records were used, scaled to PGA ranging from 0.1 g to 1.2 g, yielding a dataset of 347 seismic excitations. Three different damage indices (DIs) were used to express the seismic damage of the pier: (a) the maximum drift ratio $\delta_{r,max}$; (b) the residual drift ratio $\delta_{r,res}$; and (c) the ratio of ductility demand over ductility capacity, μ_d/μ_c. Based on the FE analysis results, three nonlinear regression models were estimated, correlating the three DIs with statistically significant IMs. The nonlinear regression model equations were evaluated in terms of various goodness-of-fit and forecasting accuracy measures, and with out-of-sample observations.

Such equations are easily programmable and can be employed for real-time damage assessment, as part of an online expert system. In the event of an earthquake, the nearest seismic motion(s), recorded by an online accelerograph network, will be used in real time to estimate the damage state of the motorway structures employing the nonlinear regression model equations. It is emphasized that the proposed method can be applied using more sophisticated FE models or a different set of IMs, and can also be applicable to other types of motorway structures.

Acknowledgement

The financial support for this paper has been provided by the research project “SYNERGY 2011” (Development of Earthquake Rapid Response System for Metropolitan Motorways) of GGET–EYDE–ETAK, implemented under the “EPAN II Competitiveness & Entrepreneurship”, co-funded by the European Social Fund (ESF) and national resources.

References

ABAQUS 6.11. (2011). Standard user's manual. Dassault Systèmes Simulia Corp., Providence, RI, USA.

Agalianos A., Sakellariadis L. (2013). *A simplified method to estimate seismic vulnerability of bridges considering soil-structure interaction.* Diploma Thesis, National Technical of Athens, Greece.

Anastasopoulos I., Gazetas G., Loli M., Apostolou M., Gerolymos N. (2010). "Soil failure can be used for seismic protection of structures" Bull Earthquake Eng (2010) 8:309–326

Anastasopoulos, P.Ch., Mannering, F.L. (2009). A note on modeling vehicle-accident frequencies with random parameter count models. Accident Analysis and Prevention, 41 (1): 153-159.

Anastasopoulos P.Ch., Mannering F.L. (2011). "An empirical assessment of fixed and random parameter logit models using crash- and non-crash-specific injury data", *Accident Analysis and Prevention*, 43 (3): 1140-1147.

Anastasopoulos, P.Ch., Shankar, V.N., Haddock, J.E., Mannering, F.L. (2012). A multivariate tobit analysis of highway accident-injury-severity rates. Accident Analysis and Prevention, 45: 110-119.

Anastasopoulos I., Sakellariadis L., Agalianos A. (2015), "Simplified method for seismic analysis of motorway bridges accounting for key structural components and nonlinear soil–structure interaction", *Soil Dynamics and Earthquake Engineering* (submitted for possible publication).

Anwaar, A., Anastasopoulos, P.Ch., Ong, G. Labi, S., Islam, M. (2012). Factors affecting highway safety, health care services, and motorization - An exploratory empirical analysis using aggregate data. Journal of Transportation Safety and Security, 4 (2): 94-115.

Applied Technology Council ATC-13 (1985). E*arthquake damage evaluation data for California*, Redwood City, California.

Applied Technology Council ATC-25 (1991). *Seismic Vulnerability and Impact of Disruption on Conterminous United States*, Redwood City, California.

Arias A. (1970). “A measure of earthquake intensity”, In: Hansen RJ (ed) *Seismic design for nuclear power plants*. MIT Press, Cambridge, pp 438–483.

Basöz N.I., Kiremidjian A.S., King S.A., Law K.H. (1999). “Statistical analysis of bridge damage data from the 1994 Northridge, CA earthquake”. *Earthquake Spectra*, 15(1):25–53.

Bertero V.V. (1977). Strength and deformation capacities of buildings under extreme environments. *Structural Engineering and Structural Mechanics*, Pister KS (ed.). Prentice Hall: Englewood Cliffs, NJ, 1977; 211–215.

Çelebi M., Sanli A., Sinclair M., Gallant S., and Radulescu D. (2004), “Real-time seismic monitoring needs of a building owner and the solution - a cooperative effort”, *Earthquake Spectra*, 20(2): 333-346, may 2004

Çelebi M. (2008), “Real-time monitoring of drift for occupancy resumption”, *Proc. 14WCEE* (CD-ROM), Beijing, China, October 13-17.

Codermatz R., Nicolich R., Slejko D. (2003). “Seismic risk assessments and GIS technology: applications to infrastructures in the Friuli-Venezia Giulia region (NE Italy)”. *Earthquake Engineering and Structural Dynamics,* Vol.32, pp. 1677-1690.

De Groeve T., Vernaccini L., Annunziato A. (2006). Global Disaster Alert and Coordination System, *Proc. 3rd International ISCRAM Conference*, Eds. B. Van de Walle and M. Turoff, Newark, pp.1-10.

EAK (2000) “Greek Seismic Code”, Organization of Seismic Planning and Protection, Athens (in Greek).

Elnashai, A., Borzi, B., and Vlachos, S., (2004). —Deformation-based Vulnerability Functions for RC Bridges, Structural Engineering and Mechanics, 17(2), 215-244.

Erdik M., Fahjan Y., Ozel O., Alcık H., Mert A., Gul M. (2003) "Istanbul earthquake rapid response and early warning system," Bulletin of Earthquake Engineering, 1(1) 157–63.

Erdik M., Sesetyan K., Demircioglu M.B., Hancilar U., Zulfikar C. (2011). "Rapid earthquake loss assessment after damaging earthquakes," Soil Dynamics and Earthquake Engineering, 31, 247–266.

FEMA (2000). Recommended seismic design criteria for new steel moment-frame buildings. *Report No. FEMA-350*, SAC Joint Venture, Federal Emergency Management Agency, Washington DC.

Franchin P., Pinto P.E. (2009). “Allowing Traffic over Mainshock-damaged Bridges”, *Journal of Earthquake Engineering*, 13(5): 585-599.

Garini E., Gazetas G. (2013). “Damage potential of near-fault records: sliding displacement against conventional “Intensity Measures””. Bull Earthquake Eng (2013) 11:455–480.

Gerolymos N., Gazetas G., Tazoh T. (2005), Seismic Response of Yielding Pile in Non-Linear Soil, *Proc. 1st Greece –Japan Workshop, Seismic Design, Observation, and Retrofit of Foundations*, pp. 25-36, Athens 11-12 October.

Hall J.F. (1995), “Northridge Earthquake of January 17, 1994 Reconnaissance Report - Volume 1”, *Earthquake Spectra*, 11.

Hanshin Expressway (1999), *Restoration of Hanshin Expressway in 623 days*, Technical Report.

Housner G.W. (1952). “Spectrum intensities of strong motion earthquakes”. Proceedings of the Symposium on earthquake and blast effects on structures, EERI, Oakland California, pp. 20–36.

Karim, K.R., Yamazaki, F. (2001). “Effect of earthquake ground motions on fragility curves of highway bridge piers based on numerical simulation”. *Earthquake Engineering and Structural dynamics*, 30: 1839-1856.

Kawashima K., Unjoh S. (1997). “The damage of highway bridges in the 1995 Hyogo-ken Nanbu earthquake and its impact on Japanese seismic design”. J*ournal of Earthquake Engineering*, 1(3): 505-541.

Kiureghian, A. D. (2002). “Bayesian Methods for Seismic Fragility Assessment of Lifeline Components”, *Acceptable Risk Processes: Lifelines and Natural Hazards*, Monograph No. 21, A. D. Kiureghian, ed., Technical Council on Lifeline Earthquake Engineering, ASCE, Reston VA USA.

Nielson B. & DesRoches R. (2007a). “Analytical Seismic Fragility Curves for Typical Bridges in the Central and Southeastern United States,” *Earthquake Spectra*, Volume 23, No. 3, pages 615–633.

Nielson B. & DesRoches R. (2007b). "Seismic fragility methodology for highway bridges using a component level approach," *Earthquake engineering and Structural Dynamics*, 36, 823–839.

Nuttli O.W. (1979). “The relation of sustained maximum ground acceleration and velocity to earthquake intensity and magnitude”. US Army Engineer Waterways Experiment Station. Miscellaneous Paper S-76-1, Report 16, p 74.

Pitilakis K., Crowley H. (2014). Recommendations for Future Directions in Fragility Function Research, *Geotechnical, Geological and Earthquake Engineering*, 27, pp. 403-413.

Pitilakis K., Crowley E., Kaynia A. (eds) (2014). *SYNER-G: Typology definition and fragility functions for physical elements at seismic risk*, ISBN 978-94-007-7872-6, Springer Science and Business Media.

Priestley M.J.N., Seible F., Calvi G.M. (1996). *Seismic design and retrofit of bridges*. Wiley, New

York.

Russo, B., Savolainen, P., Schneider, W., Anastasopoulos, P.Ch. (2014). Comparison of factors affecting injury severity in angle collisions by fault status using a random parameters bivariate ordered probit model. Analytic Methods of Accident Research, 2: 21-29.

Sarma S.K., Yang K.S. (1987), “An evaluation of strong motion records and a new parameter A95”. *Earthquake Engineering and Structural Dynamics*, 15(1): 119–132.

Shinozuka M., Feng M.Q., Lee J., and Naganuma T. (2000a). “Statistical Analysis of Fragility Curves”, *Journal of Engineering Mechanics*, 126(12): 1224-1231.

Shinozuka M., Feng M.Q., Kim H.K., and Kim S.H. (2000b). “Nonlinear Static Procedure for Fragility Curve Development”, *Journal of Engineering Mechanics*, 126(12): 1287-1295.

USC-RC (2001). “Moment-Curvature, Force-Deflection, and Axial Force-Bending Moment Interaction Analysis of Reinforced Concrete Members”. University of S. California, USA.

Vamvatsikos D., Cornell CA. (2002) “Incremental dynamic analysis Earthquake” *Earthquake Engineering and Structural Dynamics* 31 pp. 491–514.

Venkataraman, N., Shankar, V.N., Ulfarsson, G.F., Deptuch, D., 2014. A heterogeneity-in-means count model for evaluating the effects of interchange type on heterogeneous influences of interstate geometrics on crash frequencies. Analytic Methods in Accident Research, 2: 12-20.

Von Thun J.L., Rochim L.H., Scott G.A., Wilson J.A. (1988). “Earthquake ground motions for design and analysis of dams”. *Earthquake engineering and soil dynamics II—recent advances in ground-motion evaluation*. Geotechnical Special Publication 20, ASCE, pp 463–481

Washington S.P., Karlaftis M.G., Mannering F.L. (2011). *Statistical and Econometric methods for transportation data analysis*. 2nd Edition, Chapman & Hall/CRC.

Yamazaki F, Hamada T, Motoyama H, Yamauchi H. (1999). “Earthquake damage assessment of expressway bridges in Japan”. *Technical Council on Lifeline Earthquake Engineering Monograph* 1999, pp. 361-370.

Yasmin, S., Eluru, N., Bhat, C.R., Tay, R. (2014). A latent segmentation based generalized ordered logit model to examine factors influencing driver injury severity. Analytic Methods in Accident Research, 1: 23-38.

Figure 1. Structural damage of motorway bridges during: (a) the 1994 Northridge earthquake, and (b) the 1995 Kobe earthquake; (c) bus travelling on Hanshin Expressway Route No. 3 marginally stopping before a collapsed bridge span; and (d) deterioration of serviceability due to closure of road segments.

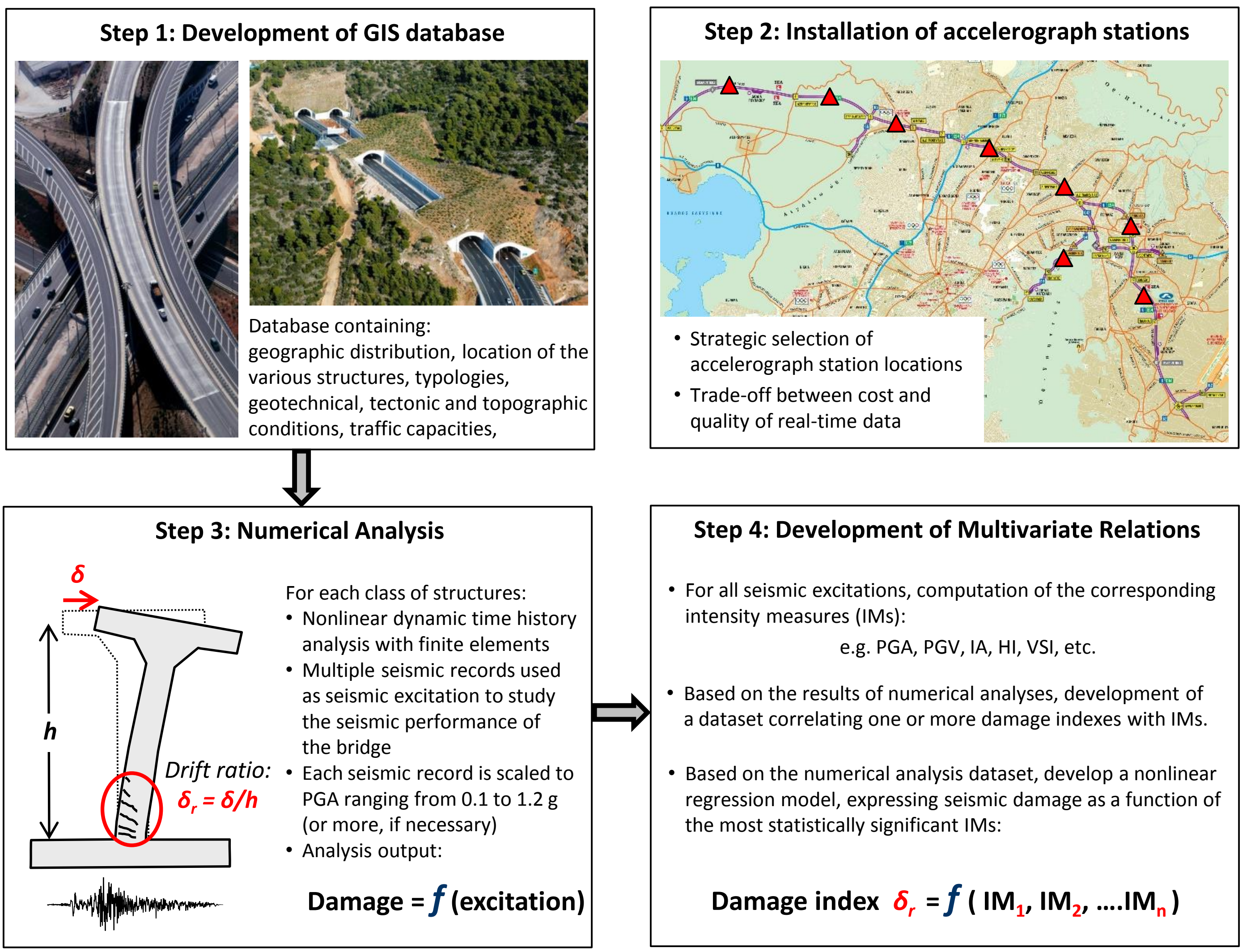

Figure 2. The four main steps required for the preparation (before the earthquake) of the RARE system.

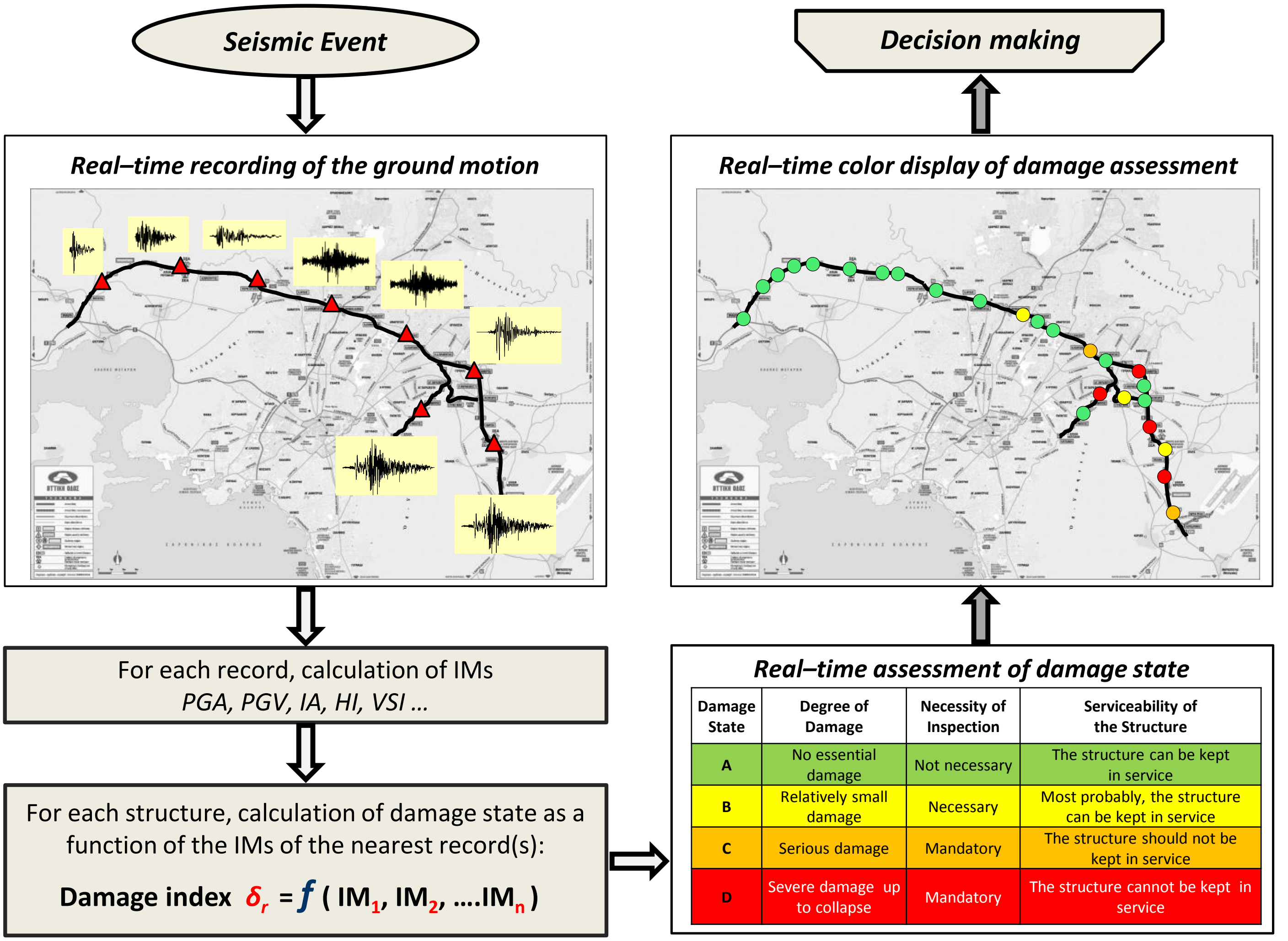

Figure 3. Schematic illustration of the application of the RARE system during a seismic event.

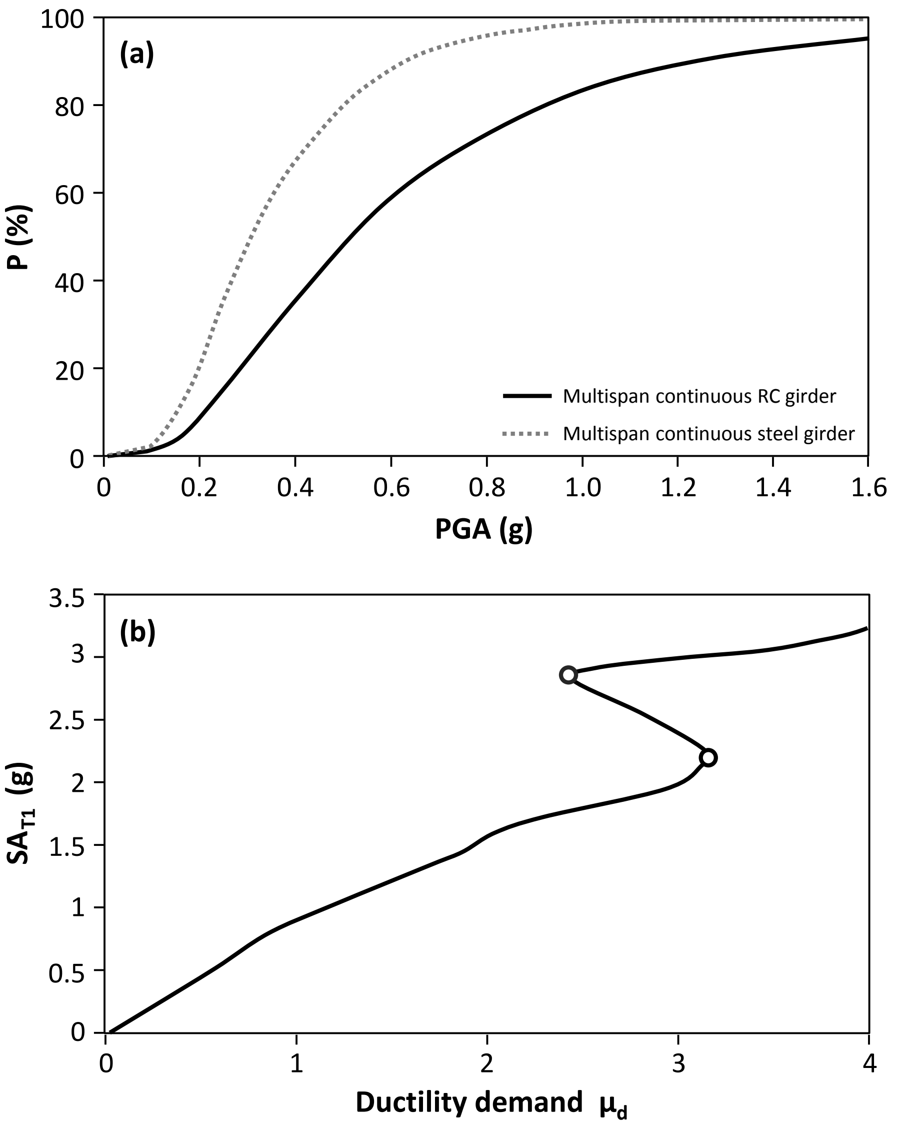

Figure 4. (a) Example of fragility curves for bridges [adapted from Nielson & DesRoches, 2007]; and (b) example of IDA (Incremental Dynamic Analysis) curve [adapted from Vamvatsikos & Cornell, 2002].

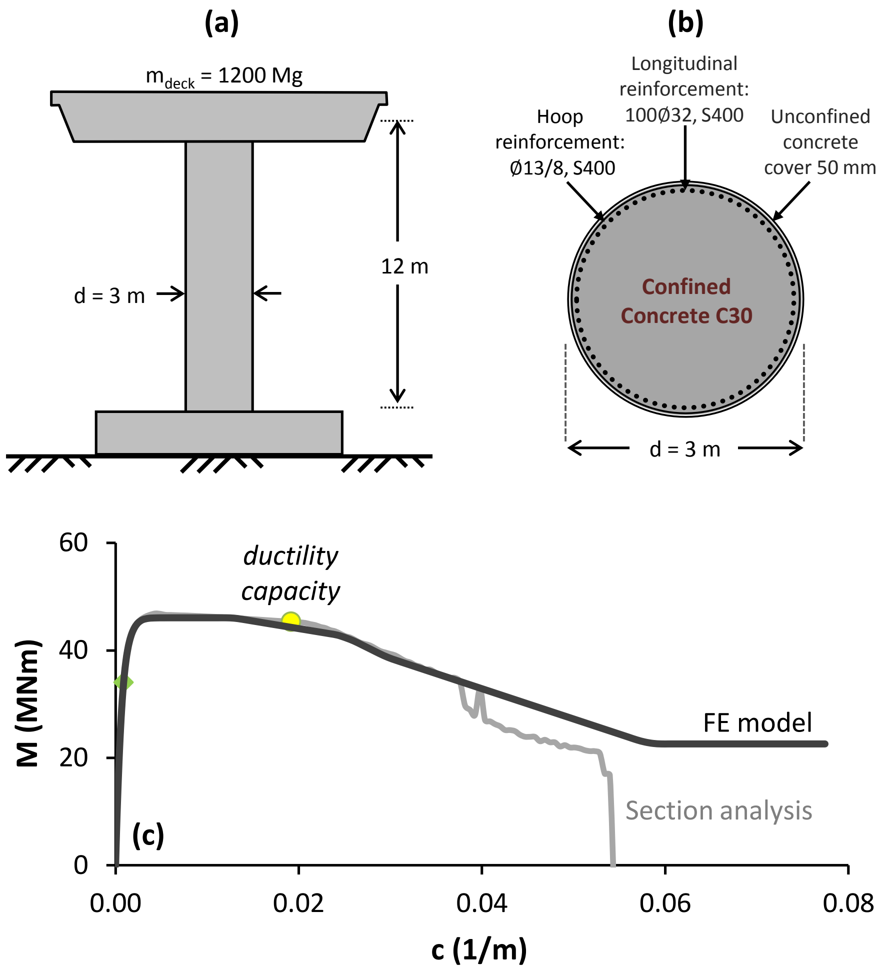

Figure 5. Bridge pier used for the analyses: (a) key characteristics; (b) pier cross-section and reinforcement details; and (c) FE model calibration against moment–curvature (*M-c*) response calculated through RC section analysis.

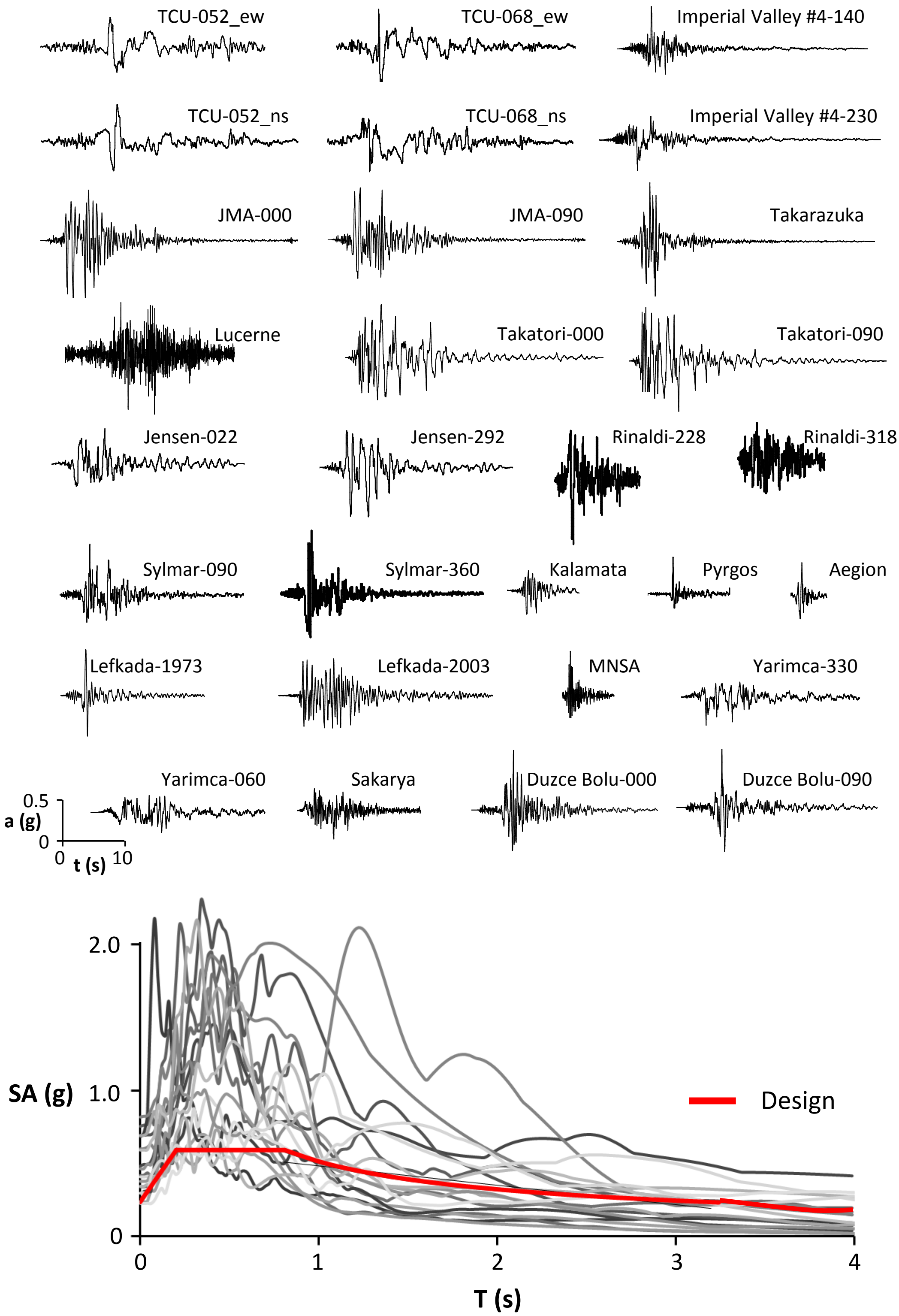

Figure 6. Real seismic records used for the analyses, along with their elastic acceleration response spectra and the design spectrum of the studied bridge.

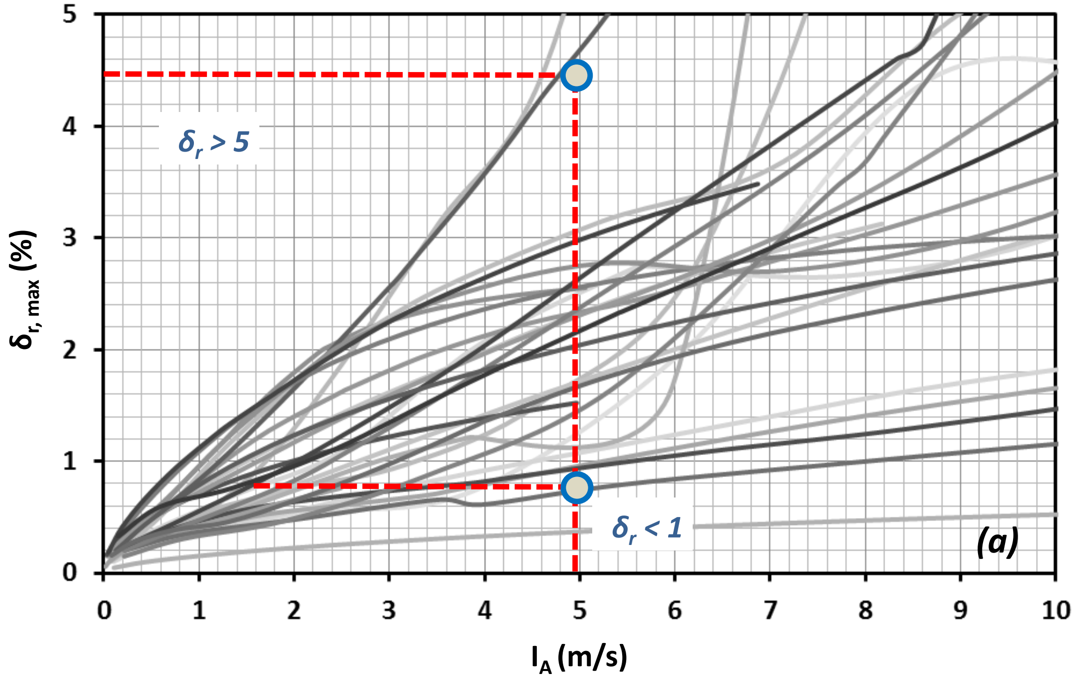

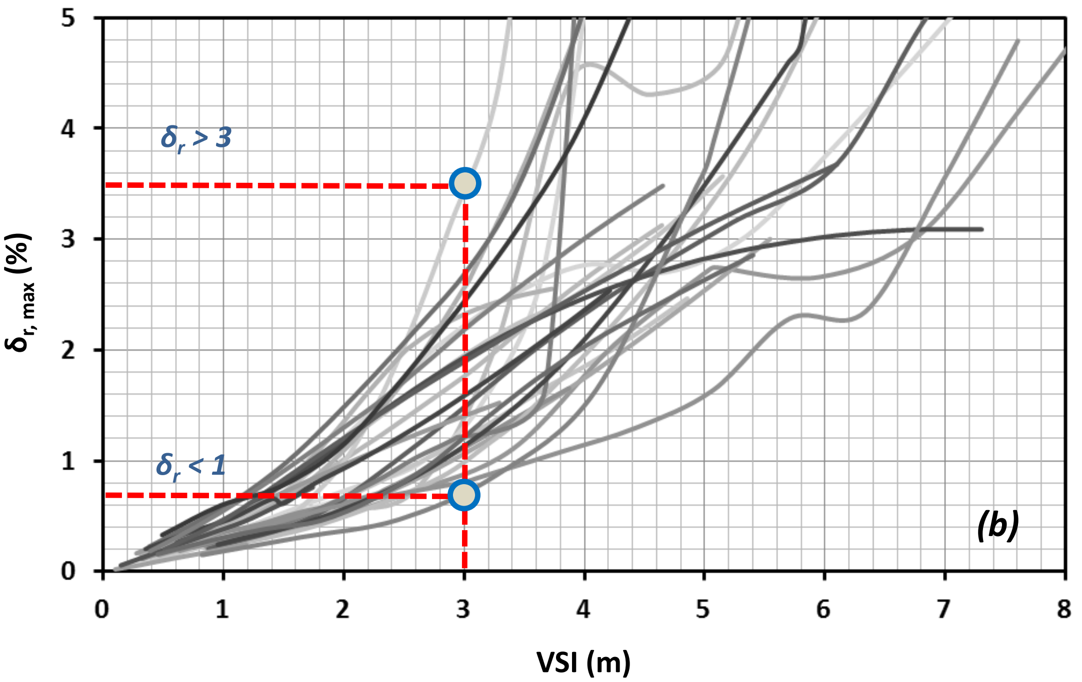

Figure 7. Correlation of $\delta_{r,max}$ as obtained from the FE analysis with: (a) I_A ; and (b) VSI.

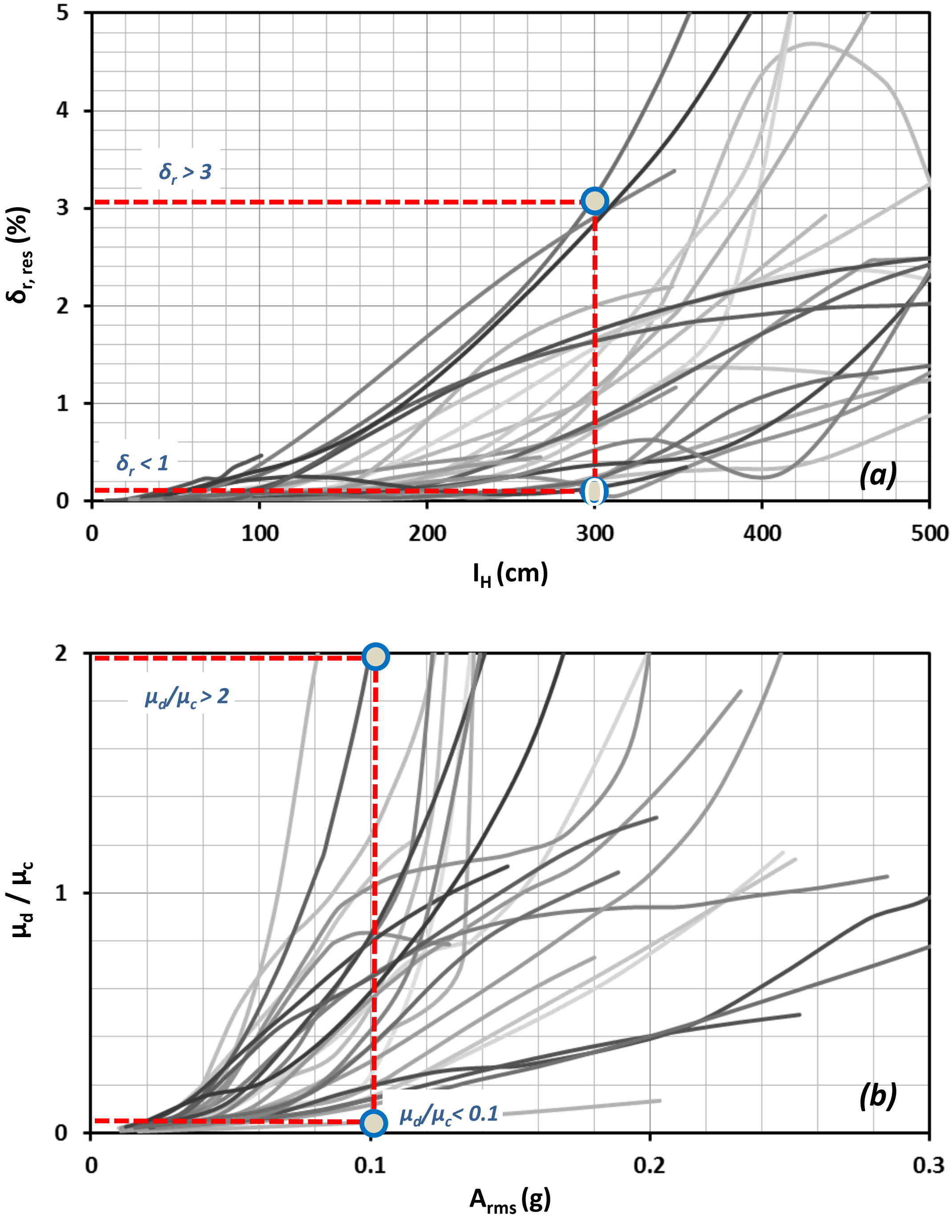

Figure 8. (a) Correlation of $\delta_{r,res}$ as obtained from the FE simulation with I_H; and (b) μ_d/μ_c as obtained from the FE simulation with A_{rms}.

	δr,max (%)	δr,res (%)	μd/μc
$R^2_{adjusted}$	0.949	0.913	0.963
MAPE	19%	69%	29%
Average Deviations	0.19	0.26	0.15

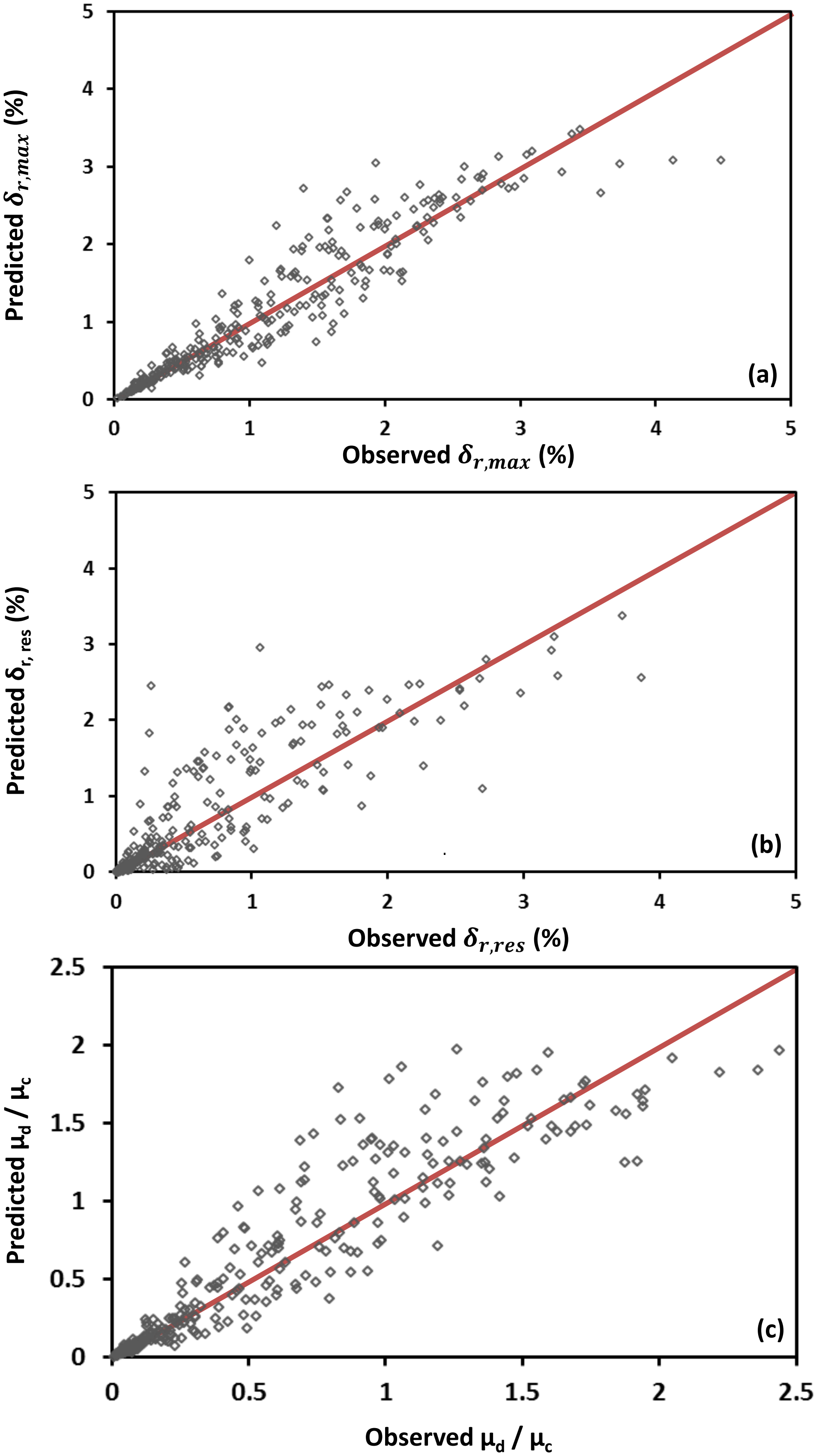

Figure 9. Observed (FE analysis) vs. predicted using the proposed nonlinear regression model equation: (a) maximum drift ratio $\delta_{r,\,max}$; (b) residual drift ratio $\delta_{r,res}$; and (c) ductility demand over ductility capacity μ_d / μ_c .

	Proposed nonlinear regression equation	
Same Damage State	292/347	84.15%
1 State difference	55/347	15.85%
2 State difference	0/347	0.00%

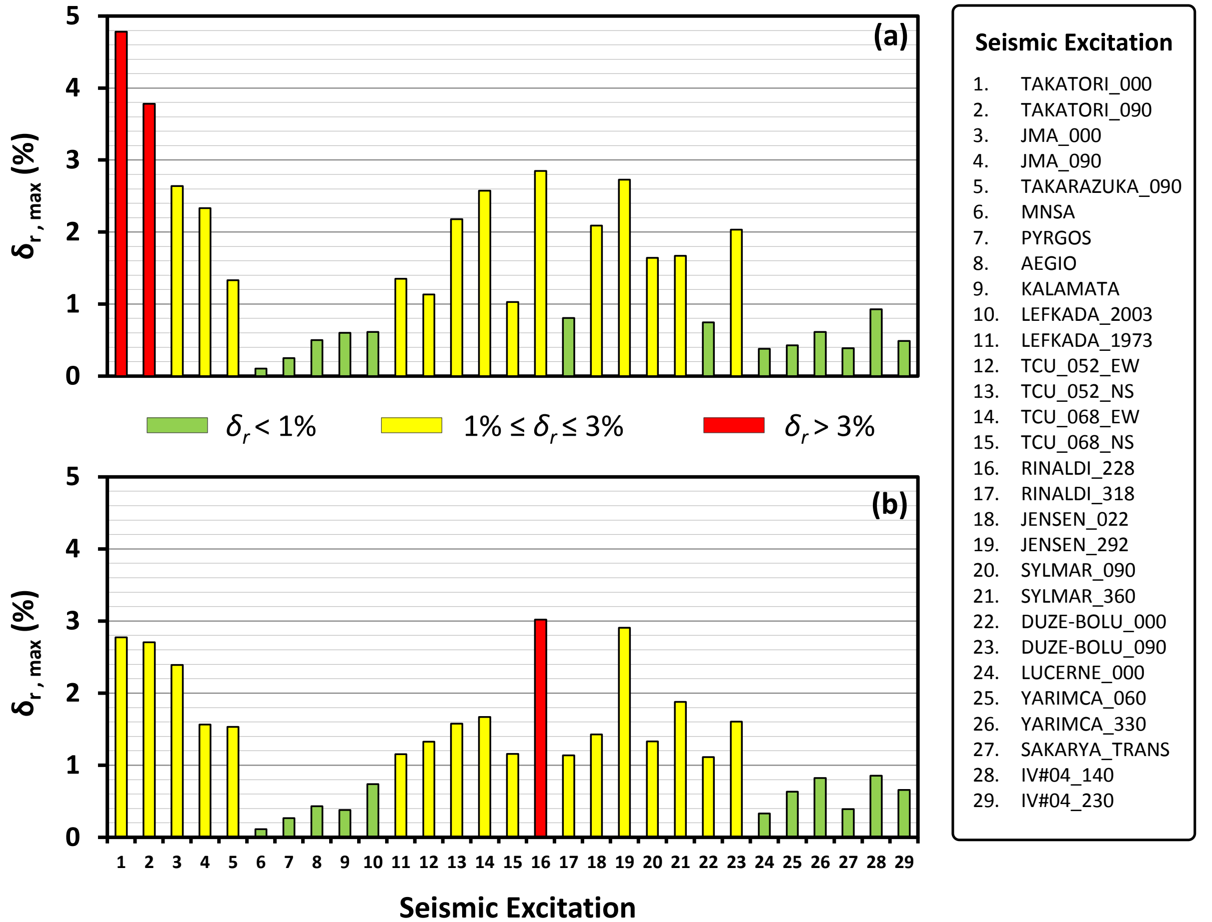

Figure 10. Comparison of (a) observed damage states based on maximum drift ratio $\delta_{r,\,max}$ of the FE analysis with (b) predicted ones based on the proposed nonlinear regression model equation for 29 historic records, and differences between predicted damage states and observed ones for 347 nonlinear dynamic analyses.

	Proposed nonlinear regression equation	
Same Damage State	281/347	80.98%
1 state Difference	60/347	17.29%
2 state Difference	6/347	1.73%

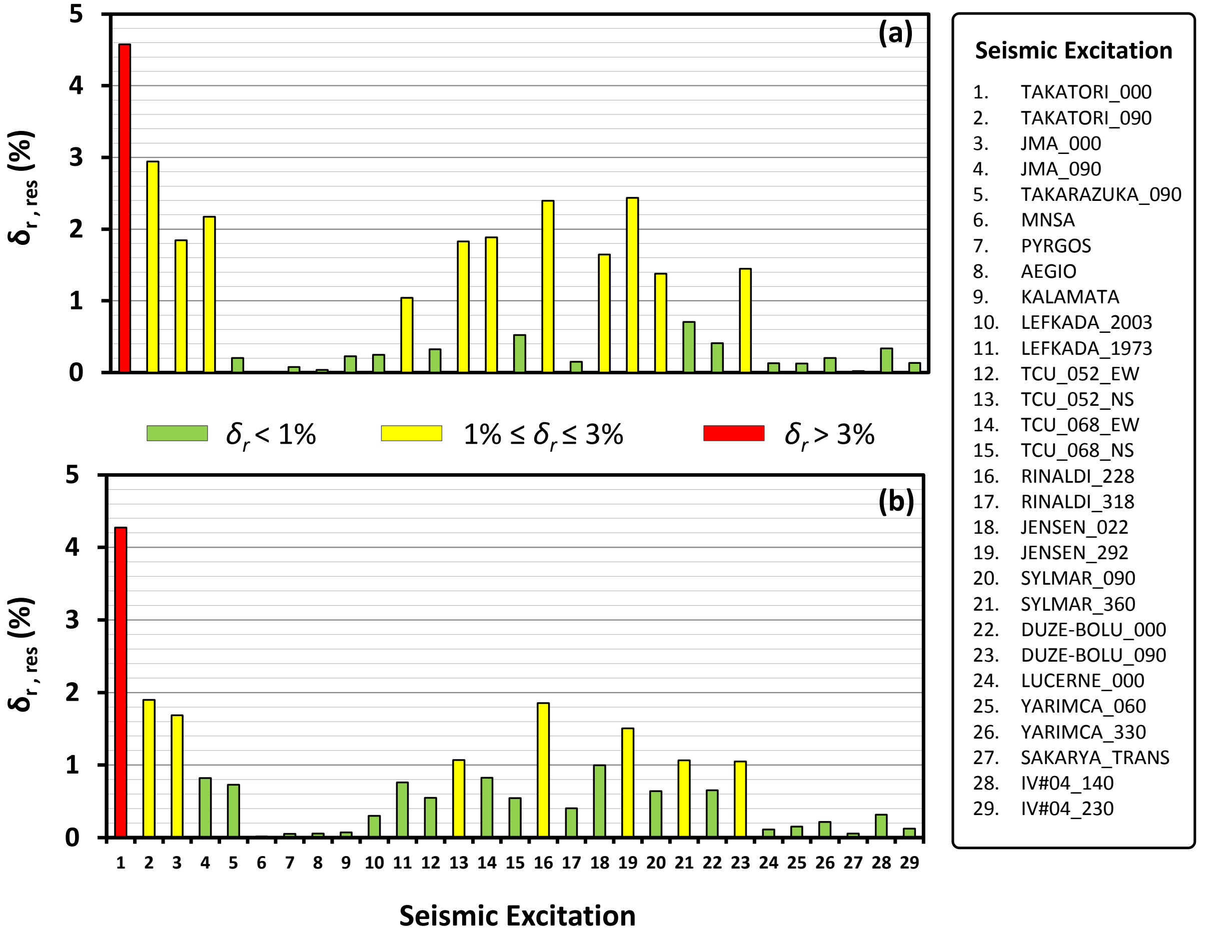

Figure 11. Comparison of (a) observed damage states based on residual drift ratio $\delta_{r,\,res}$ of the FE analysis with (b) predicted ones based on the proposed nonlinear regression model equation for 29 historic records, and differences between predicted damage states and observed ones for 347 nonlinear dynamic analyses.

	Proposed nonlinear regression equation	
Same Damage State	260/347	80.69%
1 state Difference	71/347	17.00%
2 state Difference	16/347	2.31%

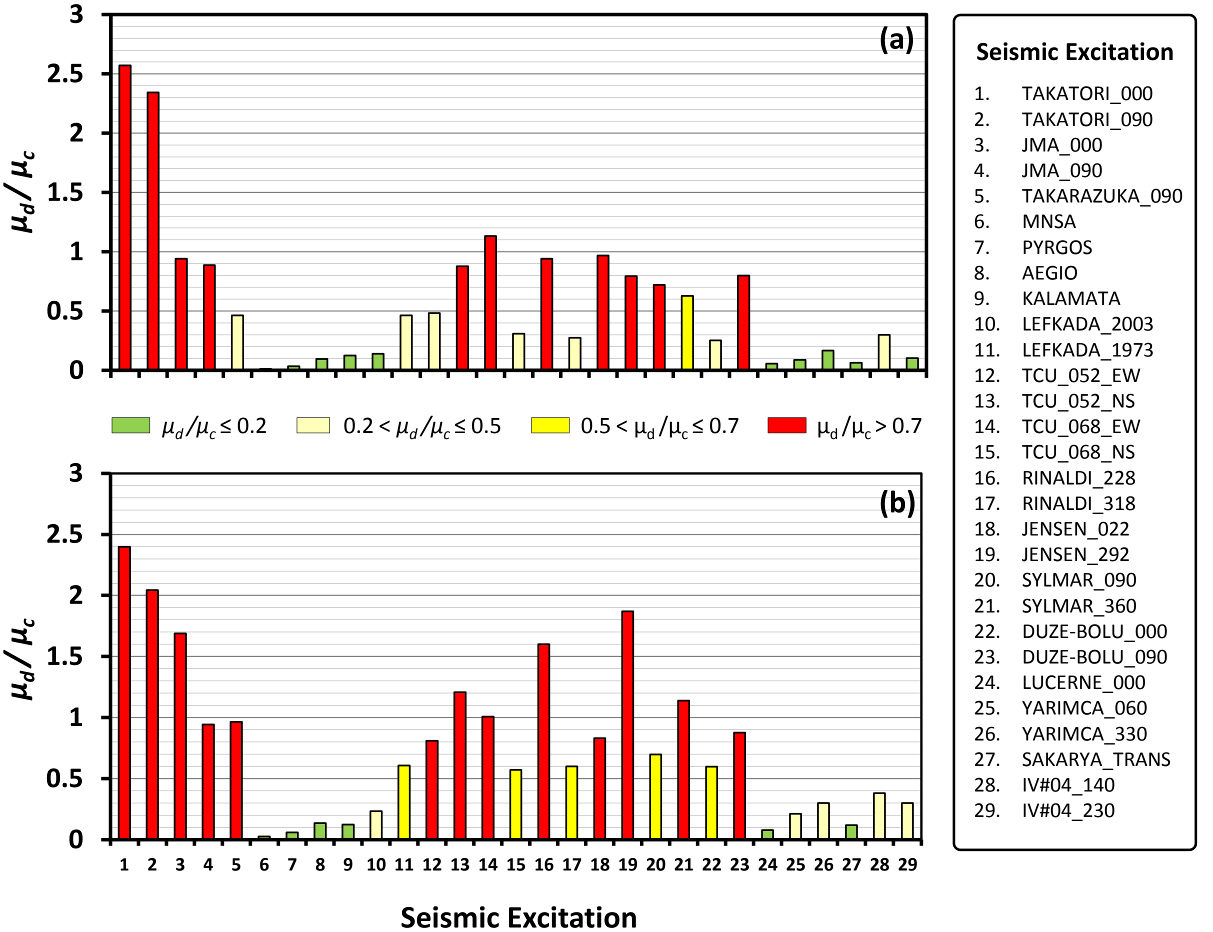

Figure 12 Comparison of (a) observed damage states based on ductility demand over ductility capacity μ_d/μ_c of the FE analysis with (b) predicted ones based on the proposed nonlinear regression model equation for 29 historic records, and differences between predicted damage states and observed ones for 347 nonlinear dynamic analyses.

	Proposed nonlinear regression equation	
Same damage state	10/15	66.67%
1 State difference	5/15	33.33%
2 State difference	0/15	0.00%

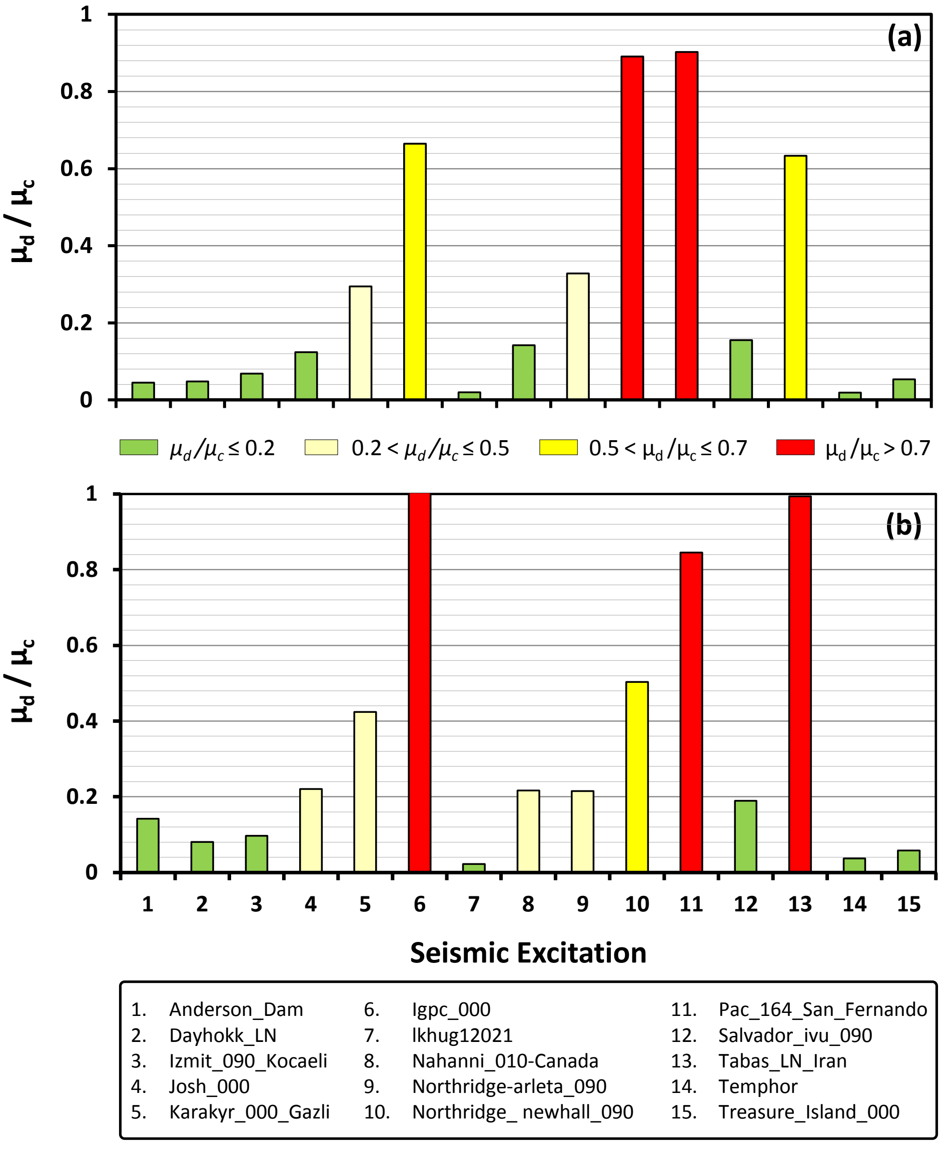

Figure 13. Comparison of (a) observed damage states based on ductility demand over ductility capacity μ_d/μ_c of the FE analysis with (b) predicted ones based on the proposed nonlinear regression model equation for 15 historic out-of-sample records, and differences between them.